Hidden Coherence Along Space-Time Trajectories in Parametric Wave Mixing

Antonio Picozzi[1] and Marc Haelterman[2]

[1]*CNRS, Laboratoire de Physique de la Matière Condensée, Université de Nice, France*
[2]*Service d'Optique et d'Acoustique, Université Libre de Bruxelles, Brussels, Belgium*

(Received 24 September 2001; published 5 February 2002)

We show theoretically that the waves generated through the generic parametric three- or four-wave-mixing processes exhibit, as a general rule, a hidden coherence characterized by skewed coherence lines along specific space-time trajectories. Our study generalizes the concept of coherence in the sense that these previously unrecognized coherent states cannot be described through the standard definitions of spatial and temporal coherence.

DOI: 10.1103/PhysRevLett.88.083901 PACS numbers: 42.65.Sf, 42.50.Ar, 42.25.Kb, 42.65.Yj

Parametric three- and four-wave-mixing processes are ubiquitous in physical sciences. They generally take place in weakly nonlinear media characterized by either quadratic or cubic nonlinearities and are thus encountered in a large variety of subfields of physics such as plasma physics, acoustics, nonlinear optics, and hydrodynamics [1]. In particular, parametric wave mixing was recently shown to be the key physical mechanism underlying the properties of Fermi resonances in multilayer superlattices [2], chiral liquid susceptibilities [3], dipolar spin waves at microwave frequencies [4], as well as interacting Bose-Einstein condensates [5]. Parametric wave mixing also makes possible coherent matter-wave amplification through the controlled interaction between a pair of light waves and a pair of matter waves [6]. Of primary importance in practice are the wave-mixing configurations in which one (or two, in the case of four-wave mixing) pump wave parametrically amplifies daughter waves that are initially incoherent (e.g., at the noise level). The fundamental problem is then to determine whether the initially incoherent daughter waves may, or not, evolve towards a coherent state during the parametric generation process.

In this Letter, we analyze mathematically and numerically the spatiotemporal coherence properties of the parametric generation and show that the daughter waves evolve, as a rule, to a specific state that contains a hidden coherence, i.e., a coherent state that can not be identified by means of the standard concepts of coherence theory. In optics, which constitutes the natural context to discuss this new coherent state, two distinct concepts of coherence are found [7]: temporal coherence refers to the ability of a field to interfere with a delayed (but not spatially shifted) version of itself, whereas spatial coherence refers to the ability of the field to interfere with a spatially shifted (but not delayed) version of itself. As we shall see, this dichotomous picture of coherence fails to describe the novel state of coherence revealed by our study of parametric wave mixing. Indeed, our analysis reveals that the parametric interaction generates fields that are self-correlated along specific spatiotemporal trajectories. In other words, the coherence of the fields is neither spatial nor temporal, but skewed in the space-time reference frame.

We present our theory in the context of nonlinear optics because parametric generation in optical media is readily accessible and thus constitutes an ideal test bed for the experimental verification of our predictions. Moreover, a distinguished feature of nonlinear optics with respect to other disciplines is the presence of noteworthy quantum effects that arise naturally from quantum fluctuations in the process of parametric generation. In this regard, our paper is relevant to quantum imaging [8], a rapidly evolving research field that deals with the concept of quantum patterns in optical parametric oscillators and amplifiers [9].

Let us consider the three- and four-wave-mixing processes in their linear regime of interaction, where the depletion of the pump waves may be neglected. The propagation of the two daughter waves of frequencies $\omega_{1,2}$ and wave numbers $k_{1,2}$ is usually studied through their slowly varying envelopes $A_{1,2}$ that obey the following linear coupled evolution equations:

$$D_1 A_1 = \kappa A_2^*, \qquad D_2 A_2 = \kappa A_1^*, \tag{1}$$

where $D_1 = \partial_z + w\partial_t + \rho\partial_y - i\eta_1\partial_{yy} - i\Delta$ and $D_2 = \partial_z - w\partial_t - \rho\partial_y - i\eta_2\partial_{yy} - i\Delta$. The parameters $w = (v_1^{-1} - v_2^{-1})/2$ and $\rho = (\rho_1 - \rho_2)/(v_1 + v_2)$ represent, respectively, the amount of velocity difference between the daughter waves $A_{1,2}$ along the longitudinal z and transverse y axes, where $\mathbf{v}_{1,2} = (v_{1,2}, \rho_{1,2})$ are the longitudinal and transverse components of the group velocities of $A_{1,2}$. The symmetric form of D_1 and D_2 with respect to these velocities is obtained by writing the equations in the reference frame traveling at the average velocity, along both the longitudinal and transverse axes. The parameters $\eta_{1,2} = 1/(2k_{1,2})$ are the diffraction coefficients of both waves and the parameter κ is the nonlinear coupling efficiency of the wave-mixing process. The parameter Δ represents the nonlinear phase shift, proportional to the pump power, that the daughter waves undergo in the case of a four-wave-mixing process.

To investigate the coherence properties of the daughter waves $A_{1,2}$ during the generation process, we shall determine the spatiotemporal autocorrelation functions $C_i(z;t,y) = \langle A_i(z,t'+t,y'+y)A_i^*(z,t',y')\rangle$ $(i = 1,2)$ (where the brackets denote integration over t' and y').

Let us recall that the spatial and temporal widths of the autocorrelation function $C_i(z;t,y)$ represent the degrees of spatial and temporal coherence of the field A_i. To calculate the autocorrelation functions $C_i(z;t,y)$ it is convenient to resort to the standard Green's function approach [10] that provides the general solution of Eq. (1) in the following form:

$$A_1 = \kappa \mathcal{G} * A_{20}^* + g_1 * A_{10}\,, \tag{2a}$$

$$A_2 = \kappa \mathcal{G}^* * A_{10}^* + g_2^* * A_{20}\,, \tag{2b}$$

where $*$ denotes the convolution product with respect to the spatial y and temporal t variables, and $A_{i0} = A_i(z = 0, t, y)$ $(i = 1, 2)$ are the initial field distributions. One can easily show that the Green's function $\mathcal{G}$ satisfies $D_1 D_2^* \mathcal{G} - \kappa^2 \mathcal{G} = \delta(z,t,y)$, where $\delta(z,t,y)$ is the 3D Dirac distribution, while the functions $g_{1,2}$ are simply deduced from $\mathcal{G}$ through $g_1 = D_2^* \mathcal{G}$, $g_2 = D_1 \mathcal{G}$. The Green's function is given by the Fourier expansion

$$\mathcal{G}(z;t,y) \propto \iint_{\mathrm{Re}^2} \exp[\gamma(\omega,q)z + i(\omega t + qy)]\, dq\, d\omega\,, \tag{3}$$

with the dispersion relation $\gamma(\omega,q) = -i\delta q^2 + [\kappa^2 - w^2(\omega + rq + \Delta/w - sq^2)^2]^{1/2}$, where $r = \rho/w$, $\delta = (\eta_1 - \eta_2)/2$, $s = \eta/w$, and $\eta = (\eta_1 + \eta_2)/2$. Since we are interested in the long term evolution of the daughter waves, the integral (3) may be calculated for large values of z by the steepest descent method [10]

$$\mathcal{G} \propto \frac{\exp(\kappa z - t^2/\tau_c^2 + i\Delta t/w)}{\sqrt{-i4(st - \delta z)}} \exp\left[-i\,\frac{(y - rt)^2}{4(st - \delta z)}\right], \tag{4}$$

where we introduced the time $\tau_c = w(2z/\kappa)^{1/2}$ that below will appear to have the physical meaning of a characteristic correlation time. Considering Eqs. (2), we can easily express the autocorrelation functions $C_i(z;t,y)$ in terms of the autocorrelation of the Green's function $C_{\mathcal{G}}(z;t,y) = \langle \mathcal{G}(z;t' + t, y' + y)\mathcal{G}^*(z;t',y')\rangle$ and the autocorrelation $C_i(z = 0,t,y)$ of the initial fields [10], which, for simplicity, we assume to be Gaussian correlated [i.e., $C_1 = C_2 = C_0(t,y) = \exp(-y^2/l_0^2 - t^2/t_0^2)/(\pi l_0 t_0)$, l_0 and t_0 being the initial correlation length and time]:

$$C_i = 2\kappa^2 C_{\mathcal{G}} * C_0 \qquad (i = 1, 2)\,. \tag{5}$$

Let us first discuss the coherence properties of $A_{1,2}$ in the limit of zero diffraction parameter, i.e., $s = \eta/w = 0$. From Eq. (5), one obtains

$$C_{1,2} \propto \exp\left[\frac{-t^2 + y^2 t_0^2/l_0^2}{2\tau_c^2(1 + r^2 t_0^2/l_0^2)}\right] \frac{\exp\left[-\frac{(y-rt)^2}{l_0^2 + r^2 t_0^2}\right]}{\sqrt{\pi(l_0^2 + r^2 t_0^2)}}\,. \tag{6}$$

Notice that this expression tends to $\exp[-t^2/(2\tau_c^2)]\delta(y - rt)$ as l_0 and t_0 tend to zero. The first factor of $C_{1,2}$ is a Gaussian whose spatial and temporal widths increase with z according to $\tau_c = w(2z/\kappa)^{1/2}$, which corresponds to an increase of spatial and temporal coherence. As regards the time dependence, this increase of coherence has been well known since the pioneering works on parametric fluorescence [11]. It is due to the temporal walk-off between the daughter waves, w, that smoothes down the initial noisy fields. However, the second factor that appears in Eq. (6) reveals a previously unrecognized fundamental aspect of parametric generation processes. Indeed, this factor [which tends to $\delta(y - rt)$ as $t_0, l_0 \to 0$] limits the extension of the correlation function to a narrow region surrounding the line $y = rt$. This means that the waves $A_{1,2}$ become coherent along specific spatiotemporal trajectories parallel to the line $y = rt$, whereas the initial incoherence remains unchanged between points that do not belong to such trajectories.

This unexpected finding has been checked by numerical simulations of Eq. (1). As shown in Fig. 1a, starting from noise the fields $A_{1,2}$ evolve to a peculiar state of coherence characterized by the presence of skewed spatiotemporal lines of correlation, in complete agreement with theory [Eq. (6)]. To interpret physically this phenomenon, we must consider the fact that the coherence of the fields appears thanks to the feedback action caused by the walk-off between the daughter waves [12]. In the framework of the present spatiotemporal analysis, the concept of walk-off is generalized to two dimensions and hence has a vector nature. The feedback action thus takes place between points belonging to lines that are parallel to the walk-off vector (i.e., in the direction of the velocity difference $\mathbf{v}_1 - \mathbf{v}_2$, as illustrated in Fig. 1b), which explains why coherence develops only along such lines. Note that the walk-off direction in the reference frame of the daughter waves' average velocity is precisely given by the straight line $y = rt$ revealed in Eq. (6) as well as in the numerical simulations (see Fig. 1a).

In the particular limit where the parameter $r = \rho/w$ tends to zero (or infinity), the interaction takes place in the absence of spatial ρ (temporal w) walk-off, and the trajectory of spatiotemporal coherence becomes parallel to the temporal (spatial) axis. It is only in these two particular cases that the coherence properties of the generated fields can be correctly described by the usual concepts of spatial and temporal coherence [7]. In the general case of skewed coherence, the use of these usual concepts would lead to

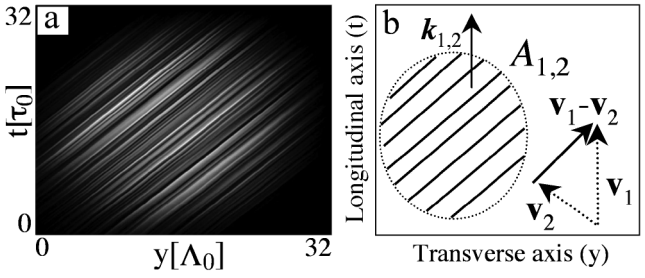

FIG. 1. (a) Spatiotemporal intensity distribution of $|A_1(t,y)|$ at $z = 11\kappa^{-1}$ in the absence of diffraction ($s = 0$) for $r = 1.95 \times 10^8$ m/s, $\kappa^{-1} = 1.88$ mm, $\Delta = 0$. The temporal and spatial units used for the normalization are $\tau_0 = w/\kappa = 0.35$ ps, $\Lambda_0 = \rho/\kappa = 68$ μm. (b) Schematic representation of the group velocities $\mathbf{v}_{1,2}$: coherence emerges along lines parallel to $\mathbf{v}_1 - \mathbf{v}_2$.

the conclusion that the field exhibits no coherence since it is neither spatial nor temporal but hidden along spatiotemporal trajectories.

Before discussing further this concept of hidden coherence, let us consider the influence of diffraction ($s \neq 0$) on the coherence of the generated waves. A typical example of the generated intensity pattern $|A_1|(t, y)$ is illustrated in Fig. 2a. Interestingly, diffraction causes the lines of coherence to cross each other, whereas they were simply juxtaposed side by side in the diffractionless case (Fig. 1a). This observation is in agreement with expression (5) of the autocorrelation function that may be easily calculated for $s \neq 0$ through an expansion in powers of t_0^2, which provides an exact expression in the form of an infinite series whose leading term is

$$C_{1,2}^{s}(z; t, y) \propto \frac{\exp[-t^2/(2\tau_c^2)]}{\sqrt{l_0^2 - 4ist}} \exp\left[-\frac{(y - rt)^2}{l_0^2 - 4ist}\right]. \quad (7)$$

Figure 2c shows that this autocorrelation function exhibits an aperture around the direction $y = rt$, a feature that naturally reflects the appearance of coherence lines of different slopes in the presence of diffraction, as revealed in Fig. 2a. For higher values of the diffraction parameter ($s > 700\ \mathrm{m^2\,s^{-1}}$) the aperture of the autocorrelation results in a drastic reduction of coherence characterized by specklelike patterns (see Fig. 2b). This effect is naturally due to the random interferences between the intersecting uncorrelated spatiotemporal lines whose slopes span the larger aperture of $|C_{1,2}^{s}(z; t, y)|$.

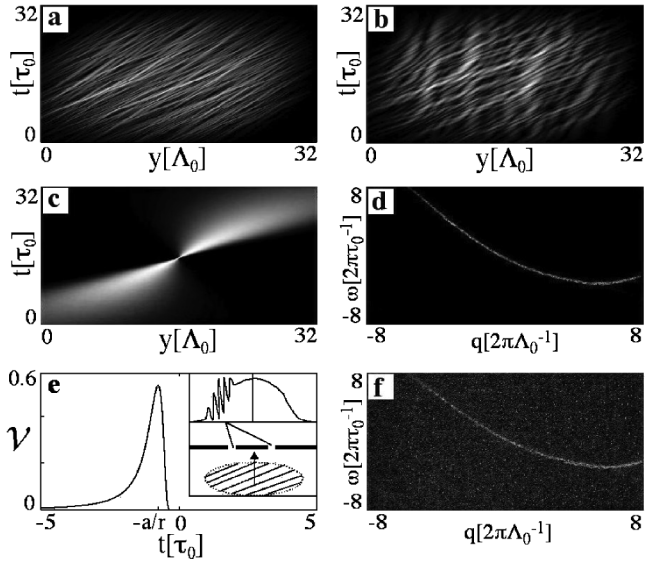

FIG. 2. Intensity distribution $|A_1(t, y)|$ for the same parameters as in Fig. 1a except that $s = 210\ \mathrm{m^2\,s^{-1}}$ (a), $s = 840\ \mathrm{m^2\,s^{-1}}$ (b). Autocorrelation function [Eq. (7)] $|C_{1,2}^{s}(t, y)|$ (c), spatiotemporal spectrum $S(\omega, q)$ (d), and respective interference fringe visibility [Eq. (9)] $\mathcal{V}(\tau)$ (inset: schematic representation of Young's experiment) (e), determined for the parameters of (a). (f) Spectrum $S(\omega, q)$ obtained below the threshold of the parametric instability.

Let us now study skewed coherence through the analysis of the spatiotemporal spectra $S(z; \omega, q)$ of the generated fields. These spectra can be easily determined from the autocorrelation function $C_{1,2}^{s}$ [7], which yields

$$S(z; \omega, q) \propto \exp[2\kappa z - \tau_c^2(\omega + rq - sq^2)^2/2] \times \tilde{C}_0(\omega, q), \quad (8)$$

where $\tilde{C}_0(\omega, q) = \exp[(-l_0^2 q^2 - t_0^2 \omega^2)/4]$ is the Fourier transform of $C_0(t, y)$. Equation (8) was found to be in excellent agreement with the spectra calculated numerically (see Fig. 2d) for a wide range of the parameters r and s. In particular, the spectra are always localized around the parabola, $\omega = -rq + sq^2$, as revealed by Eq. (8).

Let us notice that the spectra span large spatial- and temporal-frequency bandwidths, Δq and $\Delta\omega$, which, following the standard concepts of spatial and temporal coherence, would lead erroneously to the conclusion that the fields are fully incoherent. But, despite these large bandwidths, the spectra exhibit a fine two-dimensional structure (i.e., the parabola $\omega = -rq + sq^2$) that reveals the hidden coherence identified above. As s tends to zero, the spectrum reduces to a straight line of slope $-r$, which naturally corresponds to the spatiotemporal straight coherence lines found above with $s = 0$ (see Fig. 1).

This discussion reveals that the usual technique that consists of measuring the spatial and temporal spectra of a field to determine its coherence cannot be used to characterize the hidden coherence of the generated waves. It is therefore important to propose alternative techniques. In what follows we suggest a simple method aimed at providing an easy qualitative experimental demonstration of the phenomenon of skewed coherence.

This method is nothing but the classic Young's interference experiment. In this perspective, let us calculate the visibility $\mathcal{V}$ of the fringe pattern generated when making one of the daughter waves, say A_1, pass through two Young's pinholes. The visibility is determined by $\mathcal{V}(\tau) = |\Gamma_{1,2}(\tau)|/[\Gamma_{1,1}(0)\Gamma_{2,2}(0)]^{1/2}$, where $\Gamma_{1,2}(\tau) = \langle A_1(t' + \tau, y_1) A_1^*(t', y_2)\rangle$ is the mutual coherence function [7], which can be calculated explicitly by means of the Green's function Eq. (4):

$$\mathcal{V}(\tau) = \frac{\exp[-\tau^2/(2\tau_c^2)]}{(1 + 16s^2\tau^2/l_0^4)^{1/4}} \exp\left[-\frac{l_0^2(a + r\tau)^2}{l_0^4 + 16s^2\tau^2}\right], \quad (9)$$

where $a = y_2 - y_1$ is the distance between the two pinholes and τ is the time delay between the two beams coming from the two pinholes, which is proportional to the transverse spatial coordinate in the plane of observation of the fringe pattern [7]. In contrast with the usual symmetric fringe patterns encountered in Young's experiments, $\mathcal{V}(\tau)$ displays an asymmetric shape characterized by a hump localized in $\tau \simeq -a/r$ (see Fig. 2e). This asymmetry is actually the signature of the presence of skewed lines of spatiotemporal coherence: It merely reflects the ability of the daughter wave to interfere with the spatially shifted

version of itself provided it is delayed by an appropriate quantity determined by the slope r of the spatiotemporal lines of coherence, i.e., $\tau \simeq -a/r$, as indicated in Eq. (9). Note that, as the diffraction parameter s increases, the visibility $\mathcal{V}(\tau)$ of the fringes decreases and spreads in the observation plane, in agreement with the loss of coherence observed in the above study of diffraction effects (see Figs. 2a and 2b).

We draw the reader's attention to the fact that the expression of the visibility $\mathcal{V}(\tau)$ [Eq. (9)] is useful to determine the relevant experimental parameters required for the observation of the asymmetric interference patterns. More precisely, we considered for the numerical example of Fig. 2 an experimental configuration similar to that studied in Ref. [13]. In particular, the values of the parameters r and s considered in Fig. 2a correspond to a $KTiOPO_4$ crystal operating in the collinear type-II phase-matching configuration with a spatial walk-off $\rho = 35$ mrad and a temporal walk-off $w = 0.18$ ps/mm, the injected pump intensity being $I = 250$ MW/cm^2 for an effective nonlinear susceptibility of $d = 5$ pm/V and a crystal length of $L = 2.1$ cm. According to the numerical simulation reported in Figs. 2(a) and 2(e), the emergence of the skewed coherence should be easily demonstrated in Young's experiment with an asymmetric visibility $\mathcal{V}$ of up to 55% (Fig. 2e) in the standard single pass configuration starting from quantum noise fluctuations.

In summary, by means of an original theoretical treatment we analyzed the coherence properties of the parametric generation process and showed that the generated waves exhibit a hidden coherence under the form of skewed spatiotemporal coherence lines. We showed that, despite the fact that these new coherent states cannot be identified through the standard concepts of spatial and temporal coherence, they can be demonstrated by means of simple methods such as the Young's interference experiment. On the basis of the recent studies on quantum images [8,9], we can infer that our work can be pursued to explore the inherent quantum aspects associated with the vacuum field fluctuations in parametric generation. As an example, following the Langevin treatment of the dissipative parametric process driven by quantum fluctuations [9], we performed numerical simulations below the threshold of the parametric instability and observed the emergence of the characteristic parabola [Eq. (8)] in the spatiotemporal spectrum of the fields (see Fig. 2f). This spatiotemporal quantum image anticipates the formation of the skewed lines of coherence above the threshold of the instability.

Besides the context of optics, this work is relevant to many branches of nonlinear science. For instance, the coherence properties of parametrically coupled waves were shown to play a fundamental role for weakly interacting Bose gases [6], whose autocorrelation functions have been studied through the measurement of interference fringe patterns at the Bose-Einstein phase transition [14]. Considering the four-wave-mixing interaction [5], we may expect a rearrangement of matter-wave correlations along skewed lines of coherence, a feature that may be revealed by a double slit interference experiment [14], as discussed above for optical waves. Let us also mention the relevance of our work in the context of plasma physics as regards the important issue of inertial confinement fusion for which the coherence properties of the parametric instabilities were shown to be essential for the control of the confinement process [15].

The authors thank J. Botineau for fruitful discussions. The work of M. H. is supported by the Interuniversity Attraction Pole Program of the Belgian Government and the Belgian National Funds for Scientific Research.

[1] See, e.g., R. Z. Sagdeev, D. A. Usikov, and G. M. Zaslavsky, *Nonlinear Physics* (Harwood Academic, Chur, Switzerland, 1988); D. J. Kaup, A. Reiman, and A. Bers, Rev. Mod. Phys. **51**, 275 (1979).
[2] V. M. Agranovich, O. A. Dubovsky, and A. M. Kamchatnov, J. Phys. Chem. **98**, 13 607 (1994).
[3] P. Fischer *et al.,* Phys. Rev. Lett. **85**, 4253 (2000).
[4] G. A. Melkov *et al.,* Phys. Rev. Lett. **84**, 3438 (2000).
[5] L. Deng *et al.,* Nature (London) **398**, 218 (1999).
[6] S. Inouye *et al.,* Science **285**, 571 (1999); S. Inouye *et al.,* Nature (London) **402**, 641 (1999); M. Kozuma *et al.,* Science **286**, 2309 (1999).
[7] See, e.g., L. Mandel and E. Wolf, *Optical Coherence and Quantum Optics* (Cambridge University Press, New York, 1995); J. W. Goodman, *Statistical Optics* (Wiley-Interscience, New York, 1985).
[8] L. Lugiato, M. Brambilla, and A. Gatti, *Advances in Atomic, Molecular and Optical Physics,* edited by B. Bederson and H. Walther (Academic, Boston, 1999), Vol. 40.
[9] See, e.g., A. Gatti *et al.,* Phys. Rev. A **56**, 877 (1997); *ibid.*, Phys. Rev. Lett. **83**, 1763 (1999); I. Marzoli *et al.,* Phys. Rev. Lett. **78**, 2092 (1997); R. Zambrini *et al.,* Phys. Rev. A **62**, 063801 (2000).
[10] Ph. M. Morse and H. Feshbach, *Methods of Theoretical Physics* (McGraw-Hill, New York, 1953).
[11] R. L. Byer and S. E. Harris, Phys. Rev. **168**, 1064 (1968).
[12] A. Picozzi and M. Haelterman, Phys. Rev. E **63**, 056611 (2001).
[13] T. Nishikawa and N. Uesugi, J. Appl. Phys. **77**, 4941 (1995); *ibid.* **78**, 6362 (1995).
[14] I. Bloch, T. W. Hansch, and T. Esslinger, Nature (London) **403**, 166 (2000).
[15] H. Baldis and C. Labaune, Plasma Phys. Controlled Fusion **39**, 51 (1997).